HHS Public Access

Author manuscript

Cancer Cell. Author manuscript; available in PMC 2016 March 09.

Published in final edited form as:

Cancer Cell. 2015 March 9; 27(3): 397–408. doi:10.1016/j.ccell.2015.02.005.

A Functional Landscape of Resistance to ALK Inhibition in Lung Cancer

Frederick H. Wilson[1,2], **Cory M. Johannessen**[2], **Federica Piccioni**[2], **Pablo Tamayo**[2], **Jong Wook Kim**[1,2], **Eliezer M. Van Allen**[1,2], **Steven M. Corsello**[1,2], **Marzia Capelletti**[1], **Antonio Calles**[1], **Mohit Butaney**[1], **Tanaz Sharifnia**[1,2], **Stacey B. Gabriel**[2], **Jill P. Mesirov**[2], **William C. Hahn**[1,2], **Jeffrey A. Engelman**[3], **Matthew Meyerson**[1,2,4], **David E. Root**[2], **Pasi A. Jänne**[1,5], and **Levi A. Garraway**[1,2]

[1]Department of Medical Oncology, Dana-Farber Cancer Institute, Harvard Medical School, Boston, MA 02215, USA.

[2]The Broad Institute of MIT and Harvard, Cambridge, MA 02142, USA.

[3]Massachusetts General Hospital Cancer Center, Charlestown, MA 02129, USA.

[4]Department of Pathology, Brigham and Women's Hospital, Harvard Medical School, Boston, MA 02115, USA.

[5]Belfer Institute for Applied Cancer Science, Dana-Farber Cancer Institute, Harvard Medical School, Boston, MA 02215, USA.

Summary

We conducted a large-scale functional genetic study to characterize mechanisms of resistance to ALK inhibition in ALK-dependent lung cancer cells. We identify members of known resistance pathways and additional putative resistance drivers. Among the latter were members of the P2Y purinergic receptor family of G-protein coupled receptors (P2Y1, P2Y2, and P2Y6). P2Y receptors mediated resistance in part through a protein kinase C (PKC)-dependent mechanism. Moreover, PKC activation alone was sufficient to confer resistance to ALK inhibitors whereas combined ALK and PKC inhibition restored sensitivity. We observed enrichment of gene signatures associated with several resistance drivers (including P2Y receptors) in crizotinib-

Contact: To whom correspondence should be addressed: levi_garraway@dfci.harvard.edu.

Accession Numbers. RNA sequencing data are available in the dbGaP database (http://www.ncbi.nlm.nih.gov/gap) under accession number phs000855.v1.p1.

Author Contributions

F.H.W., P.A.J., and L.A.G. conceived of the project and designed the experiments. F.H.W., C.M.J., and F.P. designed and executed the primary screen and validation studies with supervision by D.E.R. T.S. assisted in the design of validation studies utilizing EGFR-mutant lung cancer cell lines under the supervision of M.M. Follow-up experimental studies were performed by F.H.W. Clinical specimens and cell lines were ascertained and processed / developed by M.C., A.C., M.B., P.A.J., and J.A.E. RNAseq data analysis was performed by F.H.W., P.T., J.W.K., E.M.V.A., and S.M.C. with oversight from L.A.G., S.B.G., J.P.M., and W.C.H. F.H.W., P.A.J., and L.A.G. wrote the manuscript.

resistant ALK-rearranged lung tumors compared to treatment-naïve controls, supporting a role for identified resistance mechanisms in clinical resistance.

Introduction

An understanding of the mechanisms by which tumors harbor primary drug resistance or acquire resistance to targeted therapies is critical for precisely predicting which patients will respond to a specific therapy and for the identification of additional targetable pathways to maximize clinical benefit (Garraway and Janne, 2012). The EML4-ALK fusion protein is an oncogenic driver in a subset of non-small cell lung cancer (NSCLC) (Soda et al., 2007). A chromosomal inversion gives rise to EML4-ALK, leading to ectopic expression of constitutively-active ALK tyrosine kinase. Aberrant ALK activity in turn up-regulates effectors of cell survival and proliferation, including the MEK/ERK and PI3K pathways (Shaw et al., 2013).

Crizotinib is an oral MET/ALK inhibitor used as first-line therapy in the treatment of advanced NSCLC harboring ALK rearrangements. In addition, newer second-generation ALK inhibitors with increased potency and selectivity against ALK are under evaluation in clinical trials. Like crizotinib, these agents are ATP-competitive inhibitors of the ALK tyrosine kinase although they are structurally distinct from crizotinib. Ceritinib (also known as LDK378) is a second-generation inhibitor that has shown remarkable activity in patients with ALK-positive lung cancer, including individuals with acquired resistance to crizotinib (Shaw et al., 2013; Shaw et al., 2014; Solomon et al., 2014). Ceritinib recently received FDA approval for use in patients with advanced ALK-rearranged NSCLC previously treated with crizotinib. However, responses to ALK inhibitors are short-lived, with resistance commonly occurring within a year.

Since the introduction of crizotinib in the treatment of ALK-driven NSCLC, gene amplification or secondary mutations in *EML4-ALK* have been identified in approximately one-third of tumors with acquired resistance to crizotinib (Choi et al., 2010; Doebele et al., 2012; Katayama et al., 2012; Sasaki et al., 2011). Secondary mutations have been shown *in vitro* to drive resistance to crizotinib, but not all confer resistance to the structurally-distinct second-generation ALK inhibitors (Katayama et al., 2011; Katayama et al., 2012). In addition, activation of EGFR, KIT, and IGF-1R have been separately identified in a subset of tumors with resistance to crizotinib (Katayama et al., 2012; Lovly et al., 2014; Sasaki et al., 2011). Resistance to second-generation ALK inhibitors is less characterized due to the recent introduction of these agents to the clinic, although secondary mutations in *EML4-ALK* have been identified in a subset of tumors with acquired ceritinib resistance (Friboulet et al., 2014). Importantly, no mechanism of resistance to crizotinib or ceritinib has been identified in up to half of all tumors reported to date (Doebele et al., 2012; Friboulet et al., 2014; Katayama et al., 2012). This observation motivates a broad search for additional resistance mediators that may provide opportunities for novel therapeutic approaches. We performed a large-scale functional genetic study to identify genes whose overexpression is sufficient to confer resistance to ALK inhibition.

Results

A large-scale functional study to identify candidate drivers of resistance to ALK inhibition

We aimed to identify gain-of-function mediators of resistance to ALK inhibition by systematic perturbation of gene expression. The Center for Cancer Systems Biology (CCSB)-Broad lentiviral expression library is a publicly-available large-scale open reading frame (ORF) library consisting of 15,885 ORFs representing 12,800 human genes (Yang et al., 2011). To identify transcripts sufficient to drive resistance to ALK inhibition, we individually introduced each ORF into an ALK-dependent lung adenocarcinoma cell line (H3122) with marked sensitivity to ALK inhibitors. ORF-expressing cells were assayed for sensitivity both to crizotinib and to the second-generation ALK inhibitor, TAE684 (Figure 1A). A mutant form (L1152R) of EML4-ALK known to confer resistance to both crizotinib and second-generation ALK inhibitors was used as a positive control (Figure 1B) (Sasaki et al., 2011). See Experimental Procedures for a full description of the experimental design.

Statistical analysis of correlation among screening replicates and estimation of lentiviral infection efficiency were performed as quality-control measures (Figure S1). 95% of assayed ORFs met quality-control thresholds and were evaluated for effects on sensitivity to ALK inhibition (see Experimental Procedures). Most ORF-expressing cells remained sensitive to crizotinib and TAE684 (Figure 1C). For H3122 cells expressing each individual ORF in the library, the differential proliferation in drug was expressed as the ratio of cell viability in the presence of drug divided by cell viability in the absence of drug. Differential proliferation for each ORF in crizotinib and TAE684 was then expressed as a z-score (% viability z-score) to normalize across the entire dataset acquired during the screen (see Experimental Procedures). ORFs conferring a differential proliferation in the presence of crizotinib or TAE684 ≥3 standard deviations (SD) above the mean (% viability z-score score ≥3) were selected as candidate mediators of resistance to ALK inhibition. A total of 75 ORFs representing 67 genes met this criterion, with 43 ORFs yielding a % viability z-score ≥3 for both drugs (Figure 1D, 2A).

Validation and characterization of candidate drivers of resistance to ALK inhibition in H3122

We next performed a validation study in which the 75 candidate ORFs were subjected to 7-point growth inhibition assays in H3122 with crizotinib and TAE684. The area under the curve (AUC) was determined for each ORF. ORFs associated with an AUC ≥2.5 SD above the mean for either drug (determined in parallel from a cohort of control ORFs) were considered validated resistance drivers in H3122. Overall, 61 ORFs representing 54 genes met this criterion (81% of candidate resistance ORFs identified from the initial screening study; Figure 2A).

Validated resistance genes reflect diverse protein classes (Figure 2B). Prominent among these are transcription factors, serine-threonine and tyrosine kinases, growth factors, and signal transduction adapter proteins. Resistance profiles of the 54 validated resistance genes against crizotinib and TAE684 in H3122 are shown in Figure 2C. Of note, we confirmed

that validated genes also drive resistance to the second-generation ALK inhibitor ceritinib with results comparable to TAE684 (Figure S2).

A subset of the identified ALK resistance genes overlap with resistance drivers to MAP kinase pathway inhibition identified in BRAF-mutant melanoma (Johannessen et al., 2010; Johannessen et al., 2013). Among these are kinases (such as AXL, MAP3K8, and RAF1), adapter proteins (including CRKL and GAB1), and transcription factors (such as ETV1, FOS, and YAP1). This finding is not surprising given the central role of MEK/ERK signaling in both contexts. However there are noteworthy differences between the datasets. For example, growth factors are more prevalent in the present study and include five EGF-related peptides (Figure S2). This is consistent with prior reports suggesting a role for EGF ligands and EGFR activation in resistance to ALK inhibition (Katayama et al., 2012; Sasaki et al., 2011; Tanimoto et al., 2014; Tanizaki et al., 2012; Voena et al., 2013; Yamada et al., 2012). More generally, these results corroborate reports implicating paracrine and autocrine mechanisms of resistance to targeted therapies (Harbinski et al., 2012; Straussman et al., 2012; Wilson et al., 2012).

We compared resistance profiles for crizotinib and TAE684 and identified three ORFs (AXL, MST1R, and HGF) that validated strongly as drivers of resistance to TAE684 (% viability z-score >5.5) but not crizotinib (% viability z-score <1; Figure 2D). This discordance likely reflects the pharmacologic activity of crizotinib against AXL, MST1R, and MET (the kinase activated by HGF) (Peters and Adjei, 2012). Similar findings for HGF-mediated resistance to ALK inhibition have been reported (Tanimoto et al., 2014; Yamada et al., 2012).

Effects of resistance ORFs on reactivation of MEK/ERK and/or PI3K pathways in H3122

Since oncogenic ALK dysregulation activates the MEK/ERK and PI3K pathways (which promote cell proliferation and survival), we next determined whether ectopically expressed resistance ORFs might confer resistance by reactivation of ERK and/or AKT in H3122 in the presence of TAE684. Approximately half of the resistance ORFs (including a subset of growth factors, kinases, and adapter proteins) produced sustained ERK and/or AKT activation despite ALK inhibition, underscoring the importance of these pathways in mediating ALK-driven tumorigenesis (Figure 3). The remaining resistance ORFs had minimal effect on these pathways, raising the possibility of resistance modules that bypass these effectors.

Assessment of validated ORFs in resistance to targeted therapies in other NSCLC cell systems

To identify resistance mechanisms more broadly operant in ALK-rearranged lung cancer, we assayed the 54 validated resistance drivers in MGH006, a second ALK-rearranged NSCLC cell line (Sequist et al., 2010). Of these, 23 conferred resistance to ALK inhibition in MGH006, as defined by a differential proliferation in drug ≥2.5 SD above the mean (determined from control ORFs) with a single dose of crizotinib or TAE684 (Experimental Procedures; Figure 4). MGH006 is reported to have a secondary dependence on EGFR activation and demonstrates reduced sensitivity to ALK inhibition compared to H3122

(Figure S3) (Katayama et al., 2012). This observation, coupled with the finding that ectopic ORF expression was generally lower in MGH006 compared to H3122 (Figure S3), suggests the resistance effects observed in MGH006 could be an underestimate. Alternatively, our findings might indicate that certain molecular contexts enable some resistance mechanisms over others.

Several ALK resistance drivers identified in H3122 (including AXL, CRKL, and HGF) have previously been implicated in resistance to EGFR inhibitors in EGFR-mutant lung cancer (Cheung et al., 2011; Engelman et al., 2007; Zhang et al., 2012). In addition, both the MEK/ERK and PI3K pathways are up-regulated by ALK or EGFR activation in lung cancer. We hypothesized that a subset of identified mediators of resistance to ALK inhibition in H3122 might also drive resistance to EGFR inhibition in EGFR-mutant lung cancer. To test this, we expressed the ALK resistance ORFs in three EGFR-mutant NSCLC lines (HCC827, HCC4006, and PC-9) and performed inhibition studies with erlotinib (Figure 4, Figure S3). Most ORFs mediating ALK resistance in H3122 also conferred resistance to erlotinib in EGFR-mutant lines, with 38 of 54 (70%) validating in at least one such line (Experimental Procedures). As the activating effects of EGF ligands are presumably blunted by EGFR inhibition, no EGF ligands identified from the ALK inhibitor screen induced resistance to erlotinib. Together, these results raise the possibility of shared mechanisms of resistance to ALK and EGFR inhibition in ALK-rearranged and EGFR-mutant lung cancers, respectively.

We evaluated expression of each resistance ORF in all 5 cell lines assayed in the initial screening and subsequent validation studies (Figure S3). The majority of assayed ORFs are expressed in all cell systems, although a subset of ORFs demonstrate differential expression across cell lines.

Neuregulin-1 as a resistance driver in ALK-dependent lung cancer cell systems

The ORF that most strongly induced resistance to ALK inhibition in both H3122 and MGH006 was neuregulin-1 (NRG1), the ligand that activates HER3. Upon ligand binding, HER3 forms heterodimers with HER2 to activate downstream signaling pathways. To confirm the ORF screening and validation findings for NRG1, we treated ALK-dependent cell lines with recombinant NRG1 peptide and assayed resistance to TAE684 (Figure 5A, B). Recombinant NRG1 peptide drives resistance to TAE684 in ALK-dependent NSCLC cell lines (H3122, H2228, and MGH006). NRG1 had no impact on sensitivity to TAE684 in KELLY cells (an ALK-dependent neuroblastoma cell line), suggesting a context-dependent role for NRG1 in driving resistance to ALK inhibition. The effect of NRG1 in ALK-dependent NSCLC cell lines was abrogated with the combination of TAE684 and lapatinib, which inhibits the activity of HER2 (the dimerization partner of HER3; Figure 5C, D). Together, these findings suggest a role for HER2/HER3 activation in resistance to ALK inhibition. Of note, NRG1 has recently been identified as a putative driver alteration in the somatic gene fusion *CD74-NRG1* in a subset of invasive mucinous lung adenocarcinoma (Fernandez-Cuesta et al., 2014).

Purinergic P2Y receptors as resistance drivers to ALK inhibition in H3122

We also examined less-characterized ALK resistance ORFs and associated pathways. Among these is P2Y2 (encoded by *P2RY2*), a member of the P2Y subfamily of P2 purinergic receptors. P2Y receptors are membrane-bound G-protein coupled receptors (GPCRs) activated in response to extracellular nucleotides including ATP. They are widely-expressed in a variety of tissues including lung epithelia (Schafer et al., 2003). A role has been postulated for P2Y receptors in mediating the activating effects of ATP in the tumor microenvironment on tumor growth (Di Virgilio, 2012). However, a role for these proteins in drug resistance has not previously been demonstrated. There are multiple P2Y family members which are further subdivided based on coupling to either Gq, Gs, or Gi (Baroja-Mazo et al., 2013). ORFs encoding ten P2Y family members are included in the CCSB-Broad lentiviral expression library. Strikingly, two additional P2Y family members (P2Y1 and P2Y6) scored highly in the initial screening study (% viability z-score 2–3) but did not meet our threshold for initial follow-up (z-score ≥3; Figure S4).

Given this observation suggesting three P2Y family members capable of impacting sensitivity to ALK inhibition in H3122, we examined these GPCRs in further detail. H3122 cells expressing these P2Y receptors demonstrated a modest but reproducible decrease in sensitivity to crizotinib in short-term assays (Figure S4). P2Y-mediated resistance was more apparent in colony-formation assays, where we observed increased survival of cells expressing P2Y receptors in crizotinib or ceritinib compared to the Lac Z control (most notably for P2Y1 and P2Y2; Figure 6A–B).

Resistance associated with P2Y receptors mediated through protein kinase C (PKC)

We sought to explore the mechanism by which P2Y receptors mediate resistance to ALK inhibition. Notably, P2Y1, P2Y2, and P2Y6 each couple to Gq to activate phospholipase C (Baroja-Mazo et al., 2013). Prior studies suggest that P2Y receptors activate phospholipase C and protein kinase C (PKC) (Falkenburger et al., 2013). More specifically, P2Y2 has been shown to activate PKCδ in intestinal cells (Amin et al., 2013). Indeed, we found that H3122 cells overexpressing P2Y1 or P2Y2 (although not P2Y6) had increased levels of activated PKCδ (Figure 6C). To determine whether PKC activation alone is sufficient to drive resistance to ALK inhibition, we treated H3122 cells with ceritinib in the presence of the PKC agonist phorbol 12-myristate 13-acetate (PMA). PMA increased the GI_{50} of ceritinib by 10-fold (Figure 6D). PKC activation also conferred resistance to ceritinib in MGH006 (Figure 6D). PMA had no impact on basal cell proliferation in the absence of ceritinib (Figure 6E). Using activated PKCδ as a marker for PKC activity, we also observed increased PKCδ activation in populations of H3122 cells cultured to resistance with ceritinib (in addition to increased EGFR activation as previously reported; Figure 6F; Figure S4; Experimental Procedures) (Katayama et al., 2012; Sasaki et al., 2011).

Sotrastaurin (AEB071) is a pan-PKC inhibitor in clinical trials (Buder et al., 2013; Chen et al., 2014). The resistance induced by PMA in H3122 and MGH006 was reversed by sotrastaurin, consistent with a PKC-dependent phenotype (Figure 6D, G). Furthermore, H3122 cells ectopically expressing P2Y receptors were sensitive to the combination of crizotinib and sotrastaurin (Figure 6H). The effect appeared specific for P2Y receptors, as

this combination did not impact resistance conferred by RAF1 (another resistance driver identified from the study; Figure 6H).

As PKCδ is not included in the CCSB-Broad ORF library, we tested whether overexpression of PKCδ (encoded by *PRKCD*) is sufficient to confer resistance to ALK inhibition in H3122. We observed that overexpression of PKCδ alone is not sufficient to induce resistance to TAE684 in our assay, suggesting that other PKC isoforms activated by PMA and inhibited by sotrastaurin may be driving the observed resistance (Figure S4). Of note, the initial screening study also identified another PKC isoform, PKCε (encoded by *PRKCE*), as sufficient to drive resistance to ALK inhibition in H3122 (Figure 2C).

Enrichment of gene signatures associated with resistance drivers in ALK inhibitor-resistant tumors compared to treatment-naive controls

We next asked whether identified resistance drivers and associated pathways might play a role in clinical resistance to ALK inhibition. We used RNAseq to generate gene expression profiles from a cohort of ALK-rearranged lung tumors with acquired resistance to crizotinib and from treatment-naïve ALK-rearranged controls (Table 1). Specimen DFCI76 harbors a secondary EML4-ALK mutation associated with crizotinib resistance (Sasaki et al., 2011); all other tumors lacked secondary ALK mutations (and activating EGFR or KRAS mutations), suggesting alternative resistance mechanisms. We used single-sample Gene Set Enrichment Analysis (ssGSEA) to query gene expression signatures for enrichment in resistant tumors compared to controls (Barbie et al., 2009; Konieczkowski et al., 2014; Subramanian et al., 2005). A total of 286 oncogenic gene signatures were evaluated, including 189 from the Molecular Signatures database (Liberzon et al., 2011). These include signatures associated with activation of a subset of resistance drivers/pathways identified from our screen, along with a P2Y signature we derived from overexpression of P2Y receptors in H3122 (Experimental Procedures; Figure 7A).

Among the gene signatures enriched in resistant tumors compared to controls (with FDR ≤0.2) were 5 signatures associated with resistance drivers/pathways identified from our functional study. Two of these were independent EGFR signatures (Creighton et al., 2006; Gatza et al., 2010; Gatza et al., 2014), consistent with prior reports of an association between EGFR activation and clinical resistance to ALK inhibition (Figure 7B). We also observed enrichment of HER2 and RAF1 signatures in resistant tumors, consistent with our findings of NRG1 (which activates HER2/HER3) and RAF1 as strong drivers of resistance to ALK inhibition (Figure 4, 5) (Creighton et al., 2006; Gatza et al., 2010; Gatza et al., 2014). Finally, the P2Y signature we identified in H3122 cells overexpressing P2Y receptors was also enriched in crizotinib-resistant tumors (Figure 7B, C; Figure S5; Table S1, S2). These findings suggest activation of transcriptional states associated with EGFR, HER2, P2Y, and RAF1 in crizotinib-resistant tumors and likely reflect underlying biological relationships between these pathways. Examination of expanded patient cohorts will be necessary to confirm these findings. Of note, many genes and pathways identified from our functional studies as resistance drivers are not represented among gene signatures used for ssGSEA analysis, limiting a computational assessment of those genes/pathways in resistant tumors compared to controls.

Given these results, we asked if transcripts encoding EGFR, HER2, RAF1, or P2Y receptors were increased in resistant tumors. Among these, expression of both *P2RY6* and *P2RY2* was significantly increased in crizotinib-resistant tumors compared to treatment-naïve controls (p=0.021 and 0.033, respectively; Figure 7D, E). This observation provides further support for activation of a P2Y gene signature in resistant tumors.

Expression signatures associated with PKC activation were not represented in the reference collection of gene signatures used for the ssGSEA analyses described above. Therefore, we queried tumor expression profiles against the compendium of expression signatures associated with chemical perturbations in the Connectivity Map (CMap) that included PKC agonists (Experimental Procedures; Table S3). Among the ALK-rearranged tumors were a relapsed post-ceritinib (DFCI133) and a pre-ceritinib (DFCI107) specimen obtained from a single patient who previously experienced disease progression on crizotinib (Table 1). Among >3200 compounds profiled in CMap, the top 3 chemical signatures most similar to DFCI133 (compared to DFCI107) were PKC agonists (Table S4). Although limited to a single patient, this preliminary observation is suggestive of PKC activation in a tumor with acquired resistance to ceritinib, consistent with our functional data. However, we did not identify a connection between gene signatures induced by PKC agonists and the entire cohort of unmatched resistant ALK-rearranged tumors compared to treatment-naïve controls.

Discussion

Patients with advanced ALK-rearranged lung cancers are treated with ALK inhibitors including crizotinib and newer second-generation inhibitors such as ceritinib or alectinib (Kwak et al., 2010; Shaw et al., 2014). As responses to these agents are generally short-lived, an understanding of the mechanisms leading to drug resistance is essential for the design of therapeutic strategies to improve efficacy. Here we present findings from a systematic large-scale functional study of resistance to ALK inhibition in ALK-rearranged lung cancer. At least 10 of the 54 ORFs identified as potential drivers of resistance to ALK inhibition represent pathways and proteins previously implicated in clinical resistance to targeted therapies in lung cancer. These include the EGFR pathway (represented by 5 EGF ligands identified from our study), MET activation (represented by HGF), SRC-related kinases (represented by FGR, LCK, and LYN), and the AXL receptor tyrosine kinase (Crystal et al., 2014; Engelman et al., 2007; Katayama et al., 2012; Zhang et al., 2012). These findings underscore the capacity of a functional genomic approach using appropriate cell line model systems to identify clinically-relevant resistance mechanisms.

Our results provide a landscape of genes capable of driving resistance to ALK inhibition and offer multiple insights about resistance pathways. A subset of the identified resistance drivers defines a signal transduction network from cell membrane to nucleus, including growth factors, receptor tyrosine kinases, adapter proteins, serine-threonine kinases, and transcription factors and DNA/RNA binding proteins. Our findings suggest that increased expression of individual genes representing multiple nodes of this signal transduction network is sufficient to drive resistance to ALK inhibition in an ALK-dependent lung cancer cell system. We demonstrate a subset of these findings is also relevant in the context of

resistance to EGFR inhibitors in EGFR-mutant lung cancer. In particular, a number of growth factors, kinases, and adapter proteins identified as ALK resistance drivers that re-activate MEK/ERK and/or PI3K signaling in H3122 also drive resistance to EGFR inhibition in EGFR-mutant lines. This finding highlights the fundamental role of these pathways in mediating the oncogenic effects of aberrant EGFR and ALK signaling.

In total, approximately half of the resistance drivers identified from our study reactivate MEK/ERK and/or PI3K signaling in H3122. Not all resistance drivers impact these pathways, however, suggesting alternative bypass mechanisms. Members of the P2Y family of purinergic receptors and downstream PKC activation represent previously unrecognized mediators of resistance to ALK inhibition. Overexpression of P2Y receptors did not impact MEK/ERK or PI3K signaling in our assays (Figure 3A, B; Figure 6C). However, there are reports suggesting a role for P2Y receptors in EGFR transactivation and MAP kinase pathway activation in other cell systems (Buvinic et al., 2007; Kehasse et al., 2013; Peterson et al., 2010; Ratchford et al., 2010; Sham et al., 2013; Tamaishi et al., 2011). The observed enrichment of gene signatures associated with EGFR, HER2, RAF1, and P2Y in crizotinib-resistant tumors may hint at shared resistance-associated transcriptional targets downstream of these pathways.

P2Y receptors mediate resistance at least in part through PKC activation. We demonstrate that PKC activation alone is sufficient to induce resistance to ALK inhibition and is overcome with combined ALK and PKC inhibition. A recent study of resistance to the BCR-ABL inhibitor imatinib in chronic myeloid leukemia revealed that up-regulation of PKCη confers resistance by activation of RAF1 and MEK/ERK signaling (Ma et al., 2014). Further work will be required to characterize the PKC isoforms driving PKC-mediated resistance in our study. In addition, larger tumor cohorts will be necessary to determine the prevalence of P2Y and/or PKC activation in clinical resistance to ALK inhibition.

In comparing resistance profiles between crizotinib and second-generation ALK inhibitors in H3122 cells, we identify HGF (which activates MET), AXL, and MST1R (also known as RON) as 3 potential mechanisms of resistance to a second-generation ALK inhibitor that do not impact sensitivity to crizotinib. As noted above, both increased MET and AXL expression has been implicated in clinical resistance to EGFR inhibitors in EGFR-mutant lung cancer (Engelman et al., 2007; Zhang et al., 2012). As crizotinib has activity against MET, AXL, and MST1R in addition to ALK, our findings suggest that crizotinib may additionally target at least 3 receptor tyrosine kinases that are potential drivers of resistance to ALK inhibition in H3122. This observation may have therapeutic implications if first-line treatment of advanced ALK-rearranged NSCLC shifts from crizotinib to more selective second-generation inhibitors that lack activity against AXL, MST1R, and MET. Conversely, recent work has shown that the second-generation ALK inhibitor ceritinib has activity against IGF-1R (in addition to ALK), which is a potential mechanism of resistance to crizotinib (Lovly et al., 2014). Thus both crizotinib and second-generation ALK inhibitors may simultaneously target distinct potential resistance drivers in addition to ALK itself.

Our findings nominate several possible agents (including inhibitors of EGFR, HER2/HER3, or PKC) that might in principle be combined with ALK inhibition to overcome or delay a

range of resistance mechanisms. However, an emerging theme from this and other comprehensive resistance studies is that activation of multiple pathways may contribute to the drug resistance phenotype (Huang et al., 2012; Johannessen et al., 2013). This poses a significant therapeutic challenge, as it may not be feasible to target all possible resistance pathways. The potential for “resistance heterogeneity” in the clinical arena may complicate identification of an optimal treatment strategy for individuals whose tumors acquire resistance to targeted therapies. Repeat biopsy at disease progression may provide an opportunity for characterization of resistant tumors to prioritize combinations for individual patients, but multiple resistance mechanisms within the same tumor could limit therapeutic efficacy (Gerlinger et al., 2012). Detailed molecular characterization of patient-derived tumors might determine the frequency at which specific resistance mechanisms occur in patients, potentially enabling prioritization of high-order therapeutic combinations for clinical trial design.

In the future, therapeutic disruption of resistance-associated transcriptional states may provide an alternative to targeting of individual upstream signaling pathways, inasmuch as such pathways might converge onto shared transcriptional outputs that drive tumor growth in drug-resistant states. Theoretically, this might be achieved by incorporation of chromatin-modifying agents as part of an ALK-directed treatment strategy. Such an approach that does not rely solely on inhibition of upstream signaling proteins susceptible to bypass might lead to more durable responses to targeted therapies.

Experimental Procedures

Cell Lines and Reagents

H3122 cells were obtained from the National Cancer Institute. Generation of ceritinib-resistant H3122 cells is described in the Supplemental Experimental Procedures. H2228, HCC827, and HCC4006 were purchased from the American Type Culture Collection (ATCC). PC-9 cells were obtained from Public Health England, and KELLY neuroblastoma cells were obtained from Sigma-Aldrich. Cells were maintained in RPMI-1640 (Cellgro) with 10% fetal bovine serum (Gemini Bioproducts) and penicillin (100 units/mL) / streptomycin (100 μg/mL; Cellgro). MGH006 cells have been previously reported and were maintained in DMEM (Cellgro) with 10% fetal bovine serum, penicillin, and streptomycin (Sequist et al., 2010). All cell lines were tested to confirm the absence of mycoplasma contamination. Crizotinib, TAE684, ceritinib, erlotinib, lapatinib, and sotrastaurin were purchased from Selleck Chemicals. Blasticidin was obtained from Life Technologies. Phorbol 12-myristate 13-acetate (PMA) was purchased from Santa Cruz Biotechnology.

Screening of the CCSB-Broad Lentiviral Expression Library

The Center for Cancer Systems Biology (CCSB)-Broad Lentiviral Expression library has been previously described (Yang et al., 2011). Additional information is included in the Supplemental Experimental Procedures. H3122 cells were seeded in white clear-bottom 384-well microtiter plates at 1500 cells per well using a Multidrop Combi (Thermo-Scientific). The next day, cells were spin-infected with the expression library (or L1152R EML4-ALK as a positive control) in the presence of 4 ug/mL polybrene at 2250 rpm for 30

minutes at 37°C. Cells were infected in 7 replicates. Virus was removed after 24 hours and replaced with standard growth media (containing 12 ug/mL blasticidin for one replicate). After an additional 48 hours, the remaining 6 replicates of ORF-expressing cells were treated with 0.01% DMSO (drug vehicle), 1 μM crizotinib, or 30 nM TAE684 (2 replicates each). Lentiviral infection, media change, and drug addition were all performed with robotics. Following 5 days of drug exposure, cell viability was determined using the Cell Titer-Glo luminescent assay (Promega) according to the manufacturer's instructions. Luminescence was measured with an EnVision Multilabel Reader (Perkin-Elmer). Screening of the entire CCSB-Broad Lentiviral Expression library (which is arrayed in forty-seven 384-well plates) was performed in 7 batches. Identification and validation of candidate resistance ORFs (and associated statistical analyses) are described in the Supplemental Experimental Procedures.

Antibodies and immunoblotting

Cells were lysed in 50 mM HEPES (pH 7.5), 1% Triton X-100, 10% glycerol, 150 mM NaCl, 2 mM EDTA, and 10 mM NaF with protease inhibitors (Roche) and phosphatase inhibitors (Calbiochem). Lysates were fractionated by SDS-polyacrylamide gel electrophoresis and transferred to nitrocellulose membranes using the iBlot system (Life Technologies). Two-color immunoblotting was performed using LI-COR reagents (Odyssey Blocking Buffer and IRDye 800CW and IRDye 680RD secondary antibodies) according to the manufacturer's instructions (LI-COR Biosciences). Fluorescence detection was performed using an Odyssey CLx Infrared Imaging System, and quantitation was performed using Image Studio software (LI-COR). Antibodies against ALK (#3791), AKT (#2920), phospho-AKT (Ser 473; #4060), EGFR (#2239), phospho-EGFR (Tyr 1068; #3777), PKCδ (#9616), and phospho-PKCδ (Tyr 311; #2055) were obtained from Cell Signaling. ERK2 antibody (sc-154) was purchased from Santa Cruz Biotechnology. Antibodies against phospho-ERK1/ERK2 (Thr 185/Tyr 187; #M8159) and vinculin (#V9131) were obtained from Sigma. V5 antibody (#R960-25) was obtained from Life Technologies. In-cell Western blotting is described in the Supplemental Experimental Procedures.

Colony-formation assays

H3122 cells were seeded in 12-well plates at a density of 10–20,000 cells per well. The following day, cells were spin-infected with lentivirus harboring the indicated ORFs in the presence of 4 μg/mL polybrene. Virus was removed after 24 hours and replaced with standard growth media. After an additional 24–48 hours, cells were treated with drug or DMSO as indicated. Cells were exposed to drug or DMSO for 14–21 days, with media change and fresh drug addition every 3 days. Cells were fixed with 4% formaldehyde and stained with 0.5% crystal violet. Cells were photographed using a Leica microscope and imaging software. Quantification of crystal violet uptake for each sample was determined by de-staining cells with 10% acetic acid and measurement of absorbance at 595 nm using a SpectraMax 190 instrument (Molecular Devices).

Whole-transcriptome sequencing (RNAseq)

Patients with ALK-rearranged NSCLC were identified from the Lowe Center for Thoracic Oncology at Dana-Farber Cancer Institute. Tumor samples were obtained under an

institutional IRB-approved protocol, and all participating patients provided written informed consent. Total RNA was extracted from fresh frozen tumor specimens using TRIzol (Life Technologies) according to the manufacturer's instructions. The presence of the *EML4-ALK* fusion transcript was confirmed by RT-PCR for each tumor.

We also prepared total RNA from H3122 cells expressing P2Y receptors for RNAseq. Parental H3122 cells or H3122 expressing ectopic Lac Z, P2Y1, or P2Y2 were exposed to 100 nM TAE684 for 12 hours. (Experimental samples were H3122 cells expressing P2Y1 or P2Y2; control samples were parental H3122 and H3122 cells expressing Lac Z.) Total RNA was extracted using the RNeasy kit (Qiagen) with on-column DNase treatment.

cDNA libraries were generated for tumor and cell line samples using the TruSeq Sample Preparation kit (Illumina) with polyA selection according to the manufacturer's protocol (Revision A 2010). Libraries were pooled using indexed adapters for multiplexing. Pooled libraries were normalized to 2 nM and denatured using 0.2 N NaOH prior to sequencing. Flowcell cluster amplification and sequencing were performed according to the manufacturer's protocols using either the HiSeq 2000 or HiSeq 2500 to a depth of 45–50 million reads per sample (paired-end with 76 base pair reads).

Data was analyzed using the Broad Picard Pipeline which includes de-multiplexing and data aggregation. Reads were mapped to the reference human genome (hg19) using TopHat 1.4.1. Expression levels for each gene were denoted as RPKM values (reads per kilobase of transcript per million mapped reads) determined using Cufflinks 2.0.2. Genes that were not expressed in any patient-derived tumor samples (RPKM=0) were removed from the tumor dataset; genes not expressed in the cell line samples were removed from the cell line dataset. Differential transcript expression was determined with the signal-to-noise test statistic with standard deviation at least 20% of the class mean. A description of the methods used to analyze RNAseq gene expression data is provided in the Supplemental Experimental Procedures.

Supplementary Material

Refer to Web version on PubMed Central for supplementary material.

Acknowledgments

We thank the patients for their participation in this study. We thank Daniel Lam, Mukta Bagul, and Thomas Nieland for technical assistance. We thank Chandra Pedamallu and Akinyemi Ojesina for assistance with processing of RNAseq data as well as Deborah Farlow and Samira Bahl for assistance in data management. We thank Ami Bhatt, David Barbie, David Takeda, Andrew Aguirre, Yaara Zwang, Rajiv Narayan, and members of the Garraway laboratory for helpful discussions. This work was supported by the Starr Cancer Consortium (L.A.G.), the National Institutes of Health (NIH) Director's New Innovator Award (DP2 0D002750, L.A.G.), NIH R01 CA136851 (P.A.J.), NIH grant T32 CA009172 (F.H.W., S.M.C.), the Huber-Foster fellowship (F.H.W.), the Conquer Cancer Foundation of ASCO Young Investigator Award (F.H.W., S.M.C.), the 2014 AACR-Bristol-Myers Squibb Oncology Fellowship in Clinical Cancer Research (Grant 14-40-15-WILS to F.H.W.), a grant from the Novartis Institute for BioMedical Research (L.A.G., W.C.H.), the National Human Genome Research Institute (NHGRI; #5U54HG003067-11; S.B.G., L.A.G.), grants from the National Cancer Institute (NCI; U54 CA112962, U01 CA176058; W.C.H.), a Career Development Award from the Melanoma Research Foundation (C.M.J.), the LINCS program (U54 HG006093), and NIH R01 CA154480 and GM074024 (J.P.M., P.T.). L.A.G. is an equity holder and consultant in Foundation Medicine. L.A.G. is a consultant to Novartis, Millenium/Takeda, and Boehringer Ingelheim and a recipient of a grant from Novartis. P.A.J. is a consultant/advisory board member for Abbot, AstraZeneca, Boehringer Ingelheim, Chugai, Clovis, Genentech, Pfizer, and Sanofi. W.C.H. is a consultant

for Novartis and recipient of a grant from Novartis. M.M. receives research support from Bayer and is an equity holder and consultant in Foundation Medicine. J.A.E. is a consultant/advisory board member of Novartis, GSK, Genentech, and AstraZeneca and a recipient of a grant from Novartis.

References

Amin R, Sharma S, Ratakonda S, Hassan HA. Extracellular nucleotides inhibit oxalate transport by human intestinal Caco-2-BBe cells through PKC-delta activation. Am J Physiol Cell Physiol. 2013; 305:C78–C89. [PubMed: 23596171]

Barbie DA, Tamayo P, Boehm JS, Kim SY, Moody SE, Dunn IF, Schinzel AC, Sandy P, Meylan E, Scholl C, et al. Systematic RNA interference reveals that oncogenic KRAS-driven cancers require TBK1. Nature. 2009; 462:108–112. [PubMed: 19847166]

Baroja-Mazo A, Barbera-Cremades M, Pelegrin P. The participation of plasma membrane hemichannels to purinergic signaling. Biochim Biophys Acta. 2013; 1828:79–93. [PubMed: 22266266]

Buder K, Gesierich A, Gelbrich G, Goebeler M. Systemic treatment of metastatic uveal melanoma: review of literature and future perspectives. Cancer Med. 2013; 2:674–686. [PubMed: 24403233]

Buvinic S, Bravo-Zehnder M, Boyer JL, Huidobro-Toro JP, Gonzalez A. Nucleotide P2Y1 receptor regulates EGF receptor mitogenic signaling and expression in epithelial cells. J Cell Sci. 2007; 120:4289–4301. [PubMed: 18057028]

Chen X, Wu Q, Tan L, Porter D, Jager MJ, Emery C, Bastian BC. Combined PKC and MEK inhibition in uveal melanoma with GNAQ and GNA11 mutations. Oncogene. 2014; 33:4724–4734. [PubMed: 24141786]

Cheung HW, Du J, Boehm JS, He F, Weir BA, Wang X, Butaney M, Sequist LV, Luo B, Engelman JA, et al. Amplification of CRKL induces transformation and epidermal growth factor receptor inhibitor resistance in human non-small cell lung cancers. Cancer Discov. 2011; 1:608–625. [PubMed: 22586683]

Choi YL, Soda M, Yamashita Y, Ueno T, Takashima J, Nakajima T, Yatabe Y, Takeuchi K, Hamada T, Haruta H, et al. EML4-ALK mutations in lung cancer that confer resistance to ALK inhibitors. N Engl J Med. 2010; 363:1734–1739. [PubMed: 20979473]

Creighton CJ, Hilger AM, Murthy S, Rae JM, Chinnaiyan AM, El-Ashry D. Activation of mitogen-activated protein kinase in estrogen receptor alpha-positive breast cancer cells in vitro induces an in vivo molecular phenotype of estrogen receptor alpha-negative human breast tumors. Cancer Res. 2006; 66:3903–3911. [PubMed: 16585219]

Crystal AS, Shaw AT, Sequist LV, Friboulet L, Niederst MJ, Lockerman EL, Frias RL, Gainor JF, Amzallag A, Greninger P, et al. Patient-derived models of acquired resistance can identify effective drug combinations for cancer. Science. 2014; 346:1480–1486. [PubMed: 25394791]

Di Virgilio F. Purines, purinergic receptors, and cancer. Cancer Res. 2012; 72:5441–5447. [PubMed: 23090120]

Doebele RC, Pilling AB, Aisner DL, Kutateladze TG, Le AT, Weickhardt AJ, Kondo KL, Linderman DJ, Heasley LE, Franklin WA, et al. Mechanisms of resistance to crizotinib in patients with ALK gene rearranged non-small cell lung cancer. Clin Cancer Res. 2012; 18:1472–1482. [PubMed: 22235099]

Engelman JA, Zejnullahu K, Mitsudomi T, Song Y, Hyland C, Park JO, Lindeman N, Gale CM, Zhao X, Christensen J, et al. MET amplification leads to gefitinib resistance in lung cancer by activating ERBB3 signaling. Science. 2007; 316:1039–1043. [PubMed: 17463250]

Falkenburger BH, Dickson EJ, Hille B. Quantitative properties and receptor reserve of the DAG and PKC branch of G(q)-coupled receptor signaling. J Gen Physiol. 2013; 141:537–555. [PubMed: 23630338]

Fernandez-Cuesta L, Plenker D, Osada H, Sun R, Menon R, Leenders F, Ortiz-Cuaran S, Peifer M, Bos M, Dassler J, et al. CD74-NRG1 Fusions in Lung Adenocarcinoma. Cancer Discov. 2014; 4:415–422. [PubMed: 24469108]

Friboulet L, Li N, Katayama R, Lee CC, Gainor JF, Crystal AS, Michellys PY, Awad MM, Yanagitani N, Kim S, et al. The ALK inhibitor ceritinib overcomes crizotinib resistance in non-small cell lung cancer. Cancer Discov. 2014; 4:662–673. [PubMed: 24675041]

Garraway LA, Janne PA. Circumventing cancer drug resistance in the era of personalized medicine. Cancer Discov. 2012; 2:214–226. [PubMed: 22585993]

Gatza ML, Lucas JE, Barry WT, Kim JW, Wang Q, Crawford MD, Datto MB, Kelley M, Mathey-Prevot B, Potti A, Nevins JR. A pathway-based classification of human breast cancer. Proc Natl Acad Sci U S A. 2010; 107:6994–6999. [PubMed: 20335537]

Gatza ML, Silva GO, Parker JS, Fan C, Perou CM. An integrated genomics approach identifies drivers of proliferation in luminal-subtype human breast cancer. Nat Genet. 2014; 46:1051–1059. [PubMed: 25151356]

Gerlinger M, Rowan AJ, Horswell S, Larkin J, Endesfelder D, Gronroos E, Martinez P, Matthews N, Stewart A, Tarpey P, et al. Intratumor heterogeneity and branched evolution revealed by multiregion sequencing. N Engl J Med. 2012; 366:883–892. [PubMed: 22397650]

Harbinski F, Craig VJ, Sanghavi S, Jeffery D, Liu L, Sheppard KA, Wagner S, Stamm C, Buness A, Chatenay-Rivauday C, et al. Rescue screens with secreted proteins reveal compensatory potential of receptor tyrosine kinases in driving cancer growth. Cancer Discov. 2012; 2:948–959. [PubMed: 22874768]

Huang S, Holzel M, Knijnenburg T, Schlicker A, Roepman P, McDermott U, Garnett M, Grernrum W, Sun C, Prahallad A, et al. MED12 controls the response to multiple cancer drugs through regulation of TGF-beta receptor signaling. Cell. 2012; 151:937–950. [PubMed: 23178117]

Johannessen CM, Boehm JS, Kim SY, Thomas SR, Wardwell L, Johnson LA, Emery CM, Stransky N, Cogdill AP, Barretina J, et al. COT drives resistance to RAF inhibition through MAP kinase pathway reactivation. Nature. 2010; 468:968–972. [PubMed: 21107320]

Johannessen CM, Johnson LA, Piccioni F, Townes A, Frederick DT, Donahue MK, Narayan R, Flaherty KT, Wargo JA, Root DE, Garraway LA. A melanocyte lineage program confers resistance to MAP kinase pathway inhibition. Nature. 2013; 504:138–142. [PubMed: 24185007]

Katayama R, Khan TM, Benes C, Lifshits E, Ebi H, Rivera VM, Shakespeare WC, Iafrate AJ, Engelman JA, Shaw AT. Therapeutic strategies to overcome crizotinib resistance in non-small cell lung cancers harboring the fusion oncogene EML4-ALK. Proc Natl Acad Sci U S A. 2011; 108:7535–7540. [PubMed: 21502504]

Katayama R, Shaw AT, Khan TM, Mino-Kenudson M, Solomon BJ, Halmos B, Jessop NA, Wain JC, Yeo AT, Benes C, et al. Mechanisms of acquired crizotinib resistance in ALK-rearranged lung Cancers. Sci Transl Med. 2012; 4:120ra117.

Kehasse A, Rich CB, Lee A, McComb ME, Costello CE, Trinkaus-Randall V. Epithelial wounds induce differential phosphorylation changes in response to purinergic and EGF receptor activation. Am J Pathol. 2013; 183:1841–1852. [PubMed: 24095926]

Konieczkowski DJ, Johannessen CM, Abudayyeh O, Kim JW, Cooper ZA, Piris A, Frederick DT, Barzily-Rokni M, Straussman R, Haq R, et al. A melanoma cell state distinction influences sensitivity to MAPK pathway inhibitors. Cancer Discov. 2014; 4:816–827. [PubMed: 24771846]

Kwak EL, Bang YJ, Camidge DR, Shaw AT, Solomon B, Maki RG, Ou SH, Dezube BJ, Janne PA, Costa DB, et al. Anaplastic lymphoma kinase inhibition in non-small-cell lung cancer. N Engl J Med. 2010; 363:1693–1703. [PubMed: 20979469]

Liberzon A, Subramanian A, Pinchback R, Thorvaldsdottir H, Tamayo P, Mesirov JP. Molecular signatures database (MSigDB) 3.0. Bioinformatics. 2011; 27:1739–1740. [PubMed: 21546393]

Lovly CM, McDonald NT, Chen H, Ortiz-Cuaran S, Heukamp LC, Yan Y, Florin A, Ozretic L, Lim D, Wang L, et al. Rationale for co-targeting IGF-1R and ALK in ALK fusion-positive lung cancer. Nat Med. 2014; 20:1027–1034. [PubMed: 25173427]

Ma L, Shan Y, Bai R, Xue L, Eide CA, Ou J, Zhu LJ, Hutchinson L, Cerny J, Khoury HJ, et al. A therapeutically targetable mechanism of BCR-ABL-independent imatinib resistance in chronic myeloid leukemia. Sci Transl Med. 2014; 6:252ra121.

Peters S, Adjei AA. MET: a promising anticancer therapeutic target. Nat Rev Clin Oncol. 2012; 9:314–326. [PubMed: 22566105]

Peterson TS, Camden JM, Wang Y, Seye CI, Wood WG, Sun GY, Erb L, Petris MJ, Weisman GA. P2Y2 nucleotide receptor-mediated responses in brain cells. Mol Neurobiol. 2010; 41:356–366. [PubMed: 20387013]

Ratchford AM, Baker OJ, Camden JM, Rikka S, Petris MJ, Seye CI, Erb L, Weisman GA. P2Y2 nucleotide receptors mediate metalloprotease-dependent phosphorylation of epidermal growth factor receptor and ErbB3 in human salivary gland cells. J Biol Chem. 2010; 285:7545–7555. [PubMed: 20064929]

Sasaki T, Koivunen J, Ogino A, Yanagita M, Nikiforow S, Zheng W, Lathan C, Marcoux JP, Du J, Okuda K, et al. A novel ALK secondary mutation and EGFR signaling cause resistance to ALK kinase inhibitors. Cancer Res. 2011; 71:6051–6060. [PubMed: 21791641]

Schafer R, Sedehizade F, Welte T, Reiser G. ATP- and UTP-activated P2Y receptors differently regulate proliferation of human lung epithelial tumor cells. Am J Physiol Lung Cell Mol Physiol. 2003; 285:L376–L385. [PubMed: 12691958]

Sequist LV, Gettinger S, Senzer NN, Martins RG, Janne PA, Lilenbaum R, Gray JE, Iafrate AJ, Katayama R, Hafeez N, et al. Activity of IPI-504, a novel heat-shock protein 90 inhibitor, in patients with molecularly defined non-small-cell lung cancer. J Clin Oncol. 2010; 28:4953–4960. [PubMed: 20940188]

Sham D, Wesley UV, Hristova M, van der Vliet A. ATP-mediated transactivation of the epidermal growth factor receptor in airway epithelial cells involves DUOX1-dependent oxidation of Src and ADAM17. PLoS One. 2013; 8:e54391. [PubMed: 23349873]

Shaw AT, Hsu PP, Awad MM, Engelman JA. Tyrosine kinase gene rearrangements in epithelial malignancies. Nat Rev Cancer. 2013; 13:772–787. [PubMed: 24132104]

Shaw AT, Kim DW, Mehra R, Tan DS, Felip E, Chow LQ, Camidge DR, Vansteenkiste J, Sharma S, De Pas T, et al. Ceritinib in ALK-rearranged non-small-cell lung cancer. N Engl J Med. 2014; 370:1189–1197. [PubMed: 24670165]

Soda M, Choi YL, Enomoto M, Takada S, Yamashita Y, Ishikawa S, Fujiwara S, Watanabe H, Kurashina K, Hatanaka H, et al. Identification of the transforming EML4-ALK fusion gene in non-small-cell lung cancer. Nature. 2007; 448:561–566. [PubMed: 17625570]

Solomon B, Wilner KD, Shaw AT. Current status of targeted therapy for anaplastic lymphoma kinase-rearranged non-small cell lung cancer. Clin Pharmacol Ther. 2014; 95:15–23. [PubMed: 24091716]

Straussman R, Morikawa T, Shee K, Barzily-Rokni M, Qian ZR, Du J, Davis A, Mongare MM, Gould J, Frederick DT, et al. Tumour micro-environment elicits innate resistance to RAF inhibitors through HGF secretion. Nature. 2012; 487:500–504. [PubMed: 22763439]

Subramanian A, Tamayo P, Mootha VK, Mukherjee S, Ebert BL, Gillette MA, Paulovich A, Pomeroy SL, Golub TR, Lander ES, Mesirov JP. Gene set enrichment analysis: a knowledge-based approach for interpreting genome-wide expression profiles. Proc Natl Acad Sci U S A. 2005; 102:15545–15550. [PubMed: 16199517]

Tamaishi N, Tsukimoto M, Kitami A, Kojima S. P2Y6 receptors and ADAM17 mediate low-dose gamma-ray-induced focus formation (activation) of EGF receptor. Radiat Res. 2011; 175:193–200. [PubMed: 21268712]

Tanimoto A, Yamada T, Nanjo S, Takeuchi S, Ebi H, Kita K, Matsumoto K, Yano S. Receptor ligand-triggered resistance to alectinib and its circumvention by Hsp90 inhibition in EML4-ALK lung cancer cells. Oncotarget. 2014; 5:4920–4928. [PubMed: 24952482]

Tanizaki J, Okamoto I, Okabe T, Sakai K, Tanaka K, Hayashi H, Kaneda H, Takezawa K, Kuwata K, Yamaguchi H, et al. Activation of HER family signaling as a mechanism of acquired resistance to ALK inhibitors in EML4-ALK-positive non-small cell lung cancer. Clin Cancer Res. 2012; 18:6219–6226. [PubMed: 22843788]

Voena C, Di Giacomo F, Panizza E, D'Amico L, Boccalatte FE, Pellegrino E, Todaro M, Recupero D, Tabbo F, Ambrogio C, et al. The EGFR family members sustain the neoplastic phenotype of ALK + lung adenocarcinoma via EGR1. Oncogenesis. 2013; 2:e43. [PubMed: 23567620]

Wilson TR, Fridlyand J, Yan Y, Penuel E, Burton L, Chan E, Peng J, Lin E, Wang Y, Sosman J, et al. Widespread potential for growth-factor-driven resistance to anticancer kinase inhibitors. Nature. 2012; 487:505–509. [PubMed: 22763448]

Yamada T, Takeuchi S, Nakade J, Kita K, Nakagawa T, Nanjo S, Nakamura T, Matsumoto K, Soda M, Mano H, et al. Paracrine receptor activation by microenvironment triggers bypass survival

signals and ALK inhibitor resistance in EML4-ALK lung cancer cells. Clin Cancer Res. 2012; 18:3592–3602. [PubMed: 22553343]

Yang X, Boehm JS, Yang X, Salehi-Ashtiani K, Hao T, Shen Y, Lubonja R, Thomas SR, Alkan O, Bhimdi T, et al. A public genome-scale lentiviral expression library of human ORFs. Nat Methods. 2011; 8:659–661. [PubMed: 21706014]

Zhang Z, Lee JC, Lin L, Olivas V, Au V, LaFramboise T, Abdel-Rahman M, Wang X, Levine AD, Rho JK, et al. Activation of the AXL kinase causes resistance to EGFR-targeted therapy in lung cancer. Nat Genet. 2012; 44:852–860. [PubMed: 22751098]

Highlights

- Multiple genes and pathways are sufficient to drive resistance to ALK inhibition
- A subset also confer resistance to EGFR inhibition in EGFR-mutant lung cancer
- P2Y receptors mediate ALK inhibitor resistance in part via protein kinase C
- EGFR, HER2, and P2Y gene signatures are enriched in crizotinib-resistant tumors

Significance

ALK inhibitors including crizotinib and ceritinib have transformed the treatment of advanced ALK-rearranged NSCLC. Unfortunately, responses to these agents are not durable, motivating efforts to characterize resistance mechanisms that inform future combinatorial treatment strategies. We assayed over 12,000 genes for the capacity to drive resistance to ALK inhibition when overexpressed in ALK-dependent lung cancer cells. Along with known resistance pathways, we identify additional resistance drivers including several P2Y purinergic receptors acting in part via protein kinase C (PKC). Collectively, our findings identify a spectrum of mechanisms sufficient to confer resistance to ALK inhibitors in NSCLC and suggest a role for P2Y receptors and PKC signaling in resistance to these agents.

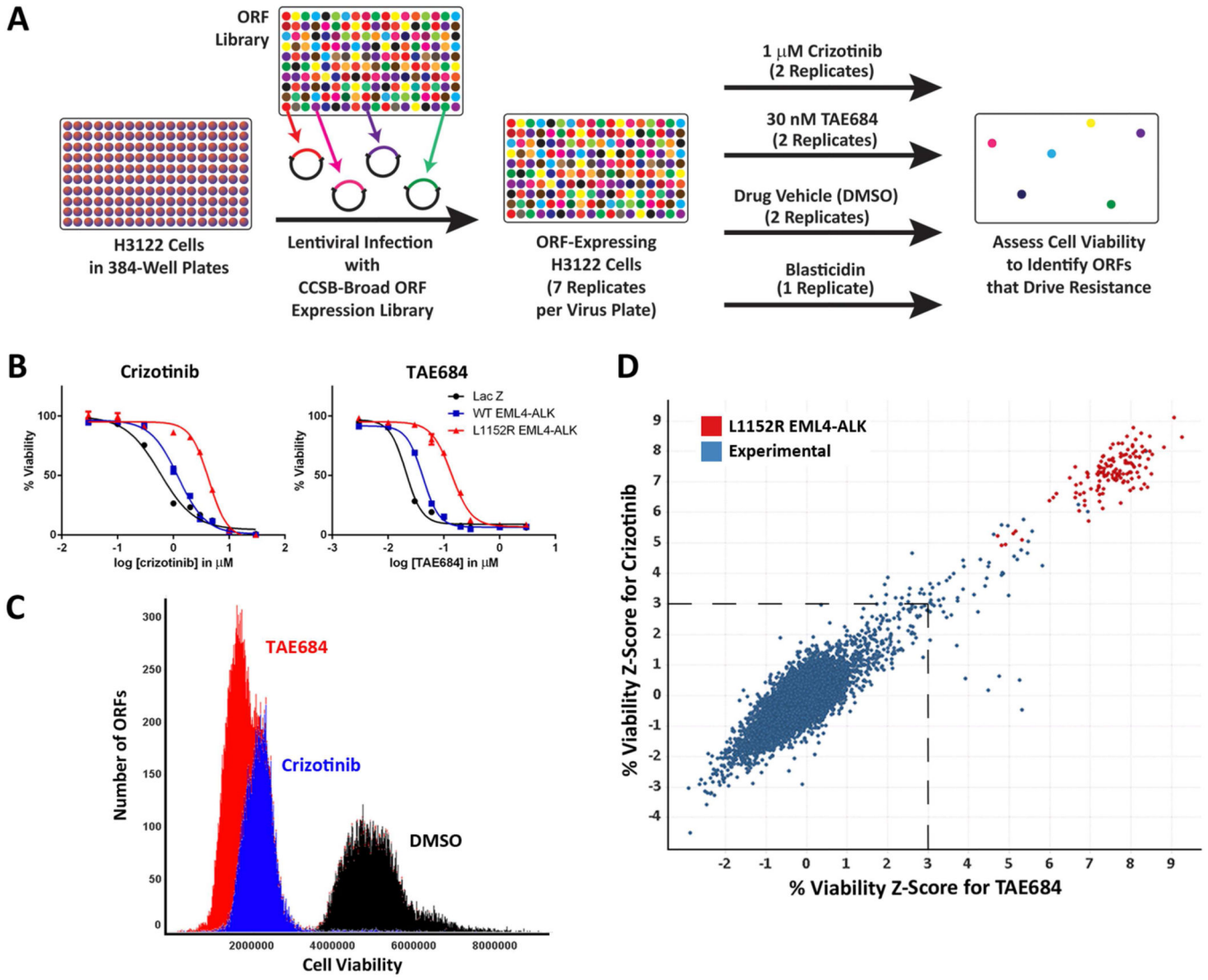

Figure 1.

A large-scale ORF screen identifies candidate mediators of resistance to ALK inhibition. **A.** Overview of the experimental approach. H3122 cells were spin-infected with the CCSB-Broad lentiviral expression library. ORF-expressing cells were then treated with crizotinib, TAE684, DMSO, or blasticidin as indicated. Cell viability was determined after 5 days of drug exposure using Cell Titer-Glo. **B.** Growth curves for H3122 cells ectopically expressing Lac Z, wild-type (WT) EML4-ALK, or L1152R EML4-ALK and exposed to crizotinib or TAE684 at varying concentrations for 5 days. Mean and standard error of 3 replicates are shown. Results are representative of 3 independent experiments. **C.** Cell viability (expressed as raw luminescence values) for all assayed ORFs in the presence or absence of drug. **D.** Percent (%) viability z-scores in the presence of crizotinib or TAE684 for each experimental ORF. % viability z-scores are defined as the normalized ratio of cell viability in drug to cell viability in drug vehicle (DMSO). % viability z-scores for replicates of the L1152R EML4-ALK positive control are shown in red. Experimental ORFs

associated with a % viability z-score ≥3 were selected as candidate mediators of resistance. See also Figure S1.

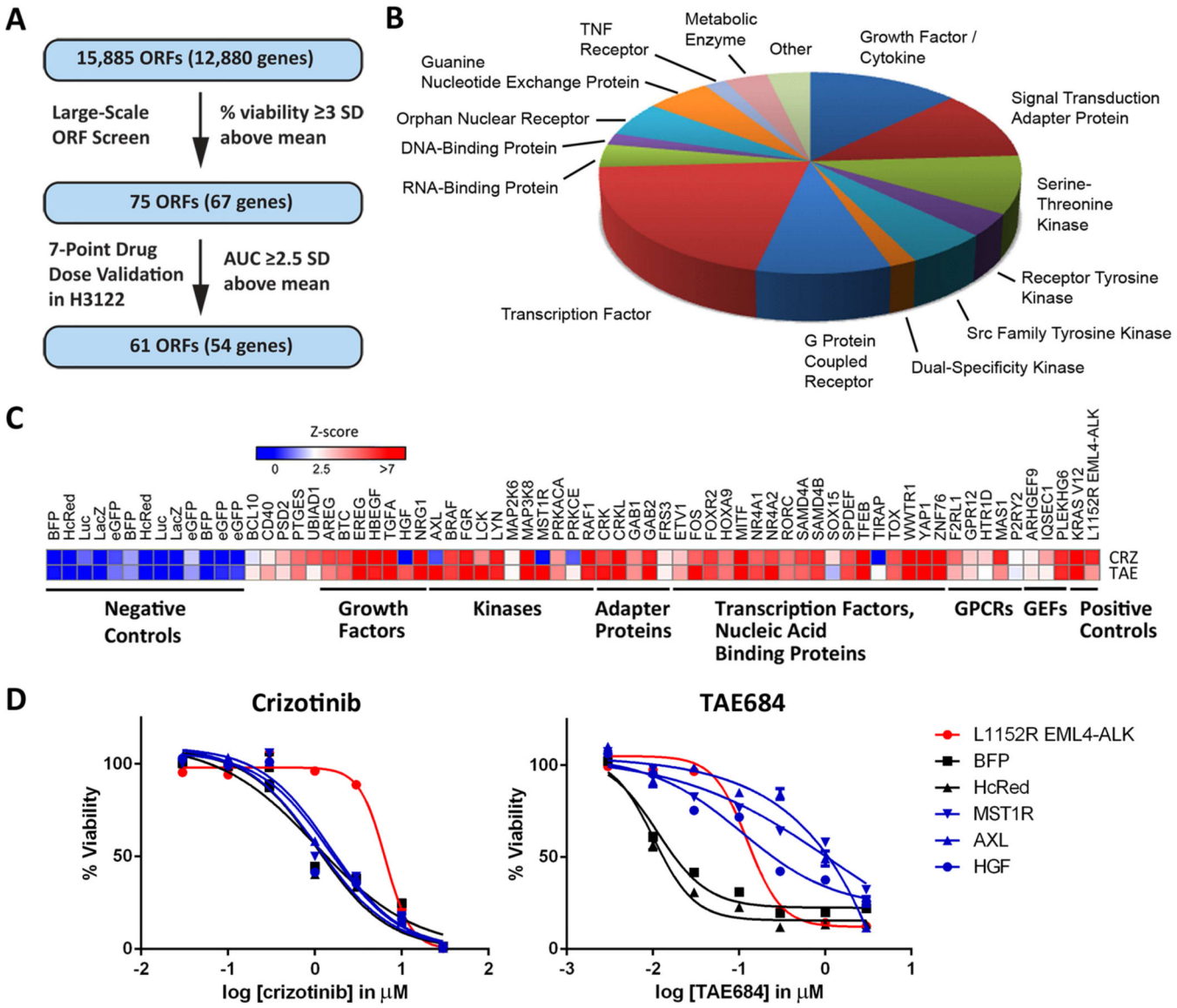

Figure 2.

Validation of candidate ORFs as drivers of resistance to ALK inhibition in H3122. **A.** Summary of initial screening and validation studies in H3122. 61 experimental ORFs (representing 54 genes) with a percent (%) viability z-score ≥3 for either drug were validated in H3122 by assessing viability of ORF-expressing cells in varying concentrations of crizotinib and TAE684. SD, standard deviation; AUC, area under the curve. **B.** Classification of the 54 genes validated as mediators of resistance in H3122. **C.** Heat map displaying normalized area under the curve (AUC) for validated drivers of resistance to crizotinib (CRZ) and TAE684 (TAE) in H3122 compared to negative controls (left). GPCRs, G-protein coupled receptors; GEFs, guanine nucleotide exchange factors. **D.** Growth curves from H3122 cells expressing MST1R, AXL, and HGF in crizotinib or TAE684. Mean and standard error of 4 replicates are shown. Growth curves of H3122 cells

expressing negative control ORFs (BFP and HcRed) and the L1152R EML4-ALK positive control are shown for comparison. See also Figure S2.

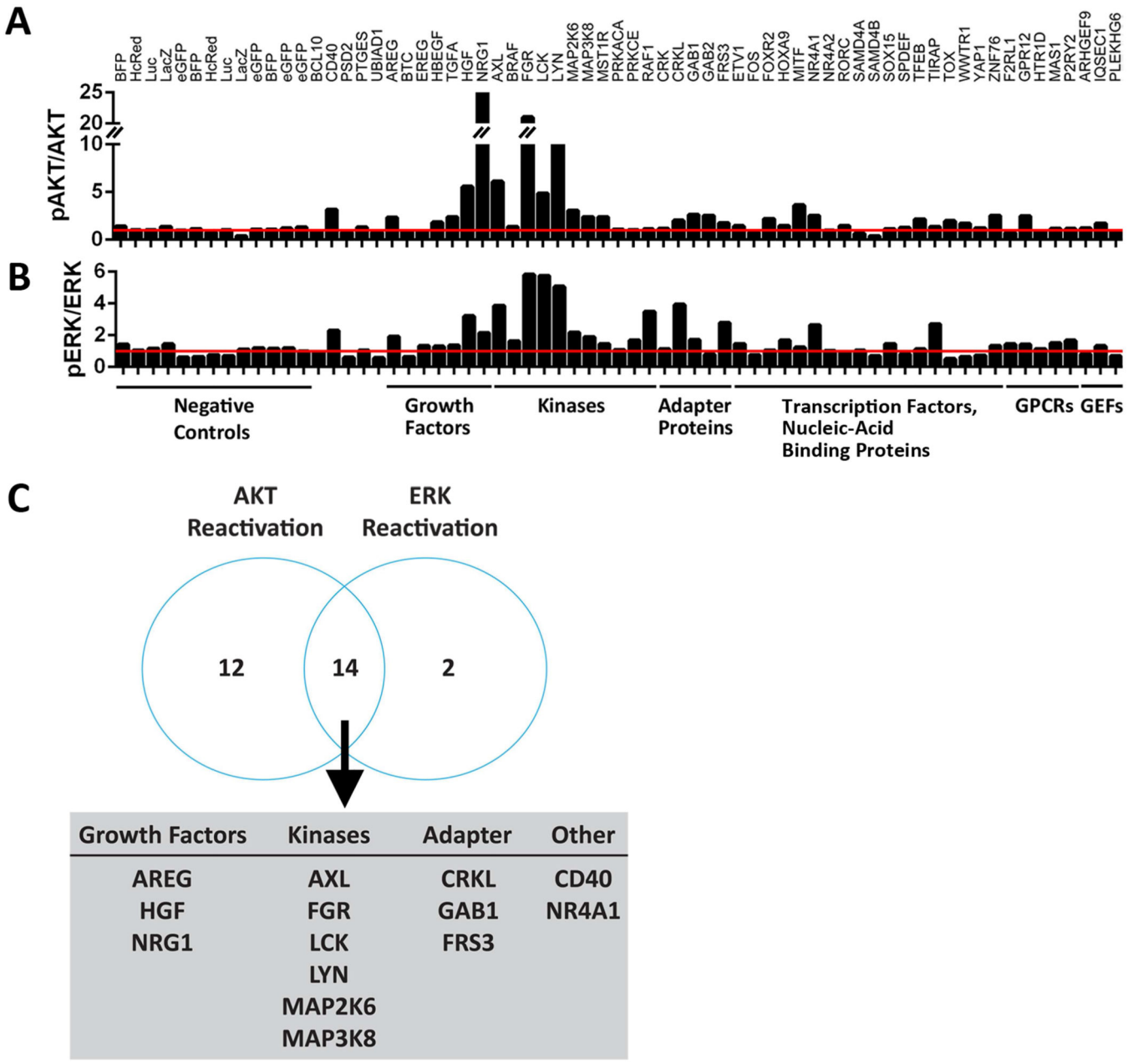

Figure 3.

A subset of validated resistance ORFs reactivate MEK/ERK or PI3K signaling. Protein lysates were prepared from ORF-expressing H3122 cells after treatment with 100 nM TAE684 for 8 hours. Immunoblotting was performed with antibodies against ERK2, phospho-ERK1/ERK2, AKT, and phospho-AKT. Fluorescence signal intensity for protein bands was quantitated. **A.** Ratio of pAKT/AKT immunostaining was determined for each ORF and normalized to mean pAKT/AKT determined from 13 negative controls (left). Fold-increase in pAKT/AKT relative to controls is shown, with the red horizontal line representing mean pAKT/AKT from controls. **B.** As in A, except with pERK/ERK. GPCRs, G-protein coupled receptors; GEFs, guanine nucleotide exchange factors. **C.** Venn diagram

demonstrating overlap between ORFs reactivating AKT or ERK. Resistance ORFs associated with a pAKT/AKT or pERK/ERK ratio ≥2.5 standard deviations above the mean (as determined from the negative controls) were designated as ORFs reactivating AKT or ERK in the presence of TAE684, respectively. 28 of 54 resistance ORFs (52%) met this criteria for AKT or ERK; 14 of these 28 ORFs were associated with reactivation of both AKT and ERK and are indicated in the shaded box.

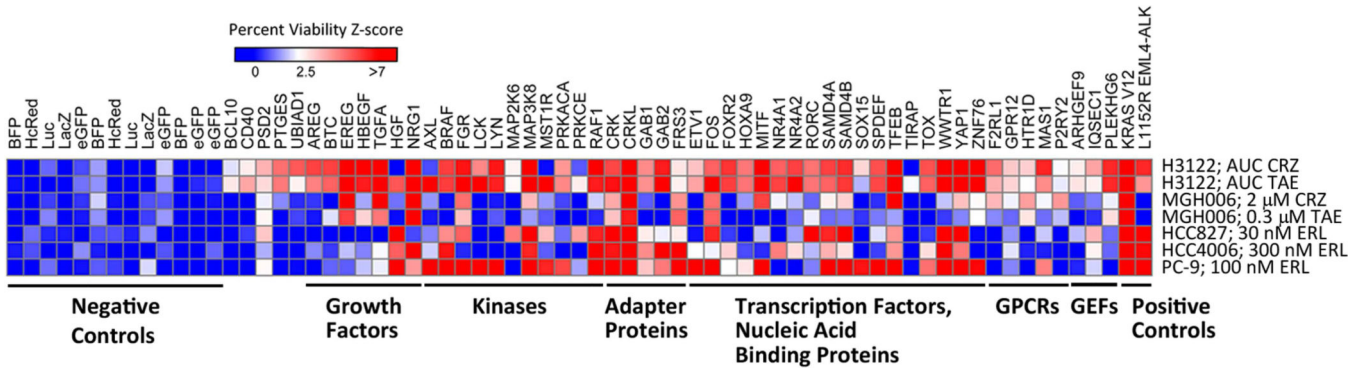

Figure 4.

A subset of resistance ORFs identified in H3122 also drive resistance to targeted therapies in other lung cancer cell systems. Heat map displaying normalized area under the curve (AUC) for validated drivers of resistance to crizotinib (CRZ) and TAE684 (TAE) in H3122 compared to negative controls (left) as in Figure 2C. Normalized percent viability for ORF-expressing cells in the indicated doses of CRZ or TAE (for MGH006) or erlotinib (ERL; for HCC827, HCC4006, and PC-9) are shown. Relative expression of each ectopic experimental ORF in each cell line is shown in Figure S3. Of note, we were unable to demonstrate ectopic expression of L1152R EML4-ALK in MGH006 (data not shown), and no effect of this positive control ORF was therefore observed on resistance to ALK inhibition in MGH006. GPCRs, G-protein coupled receptors; GEFs, guanine nucleotide exchange factors. See also Figure S3.

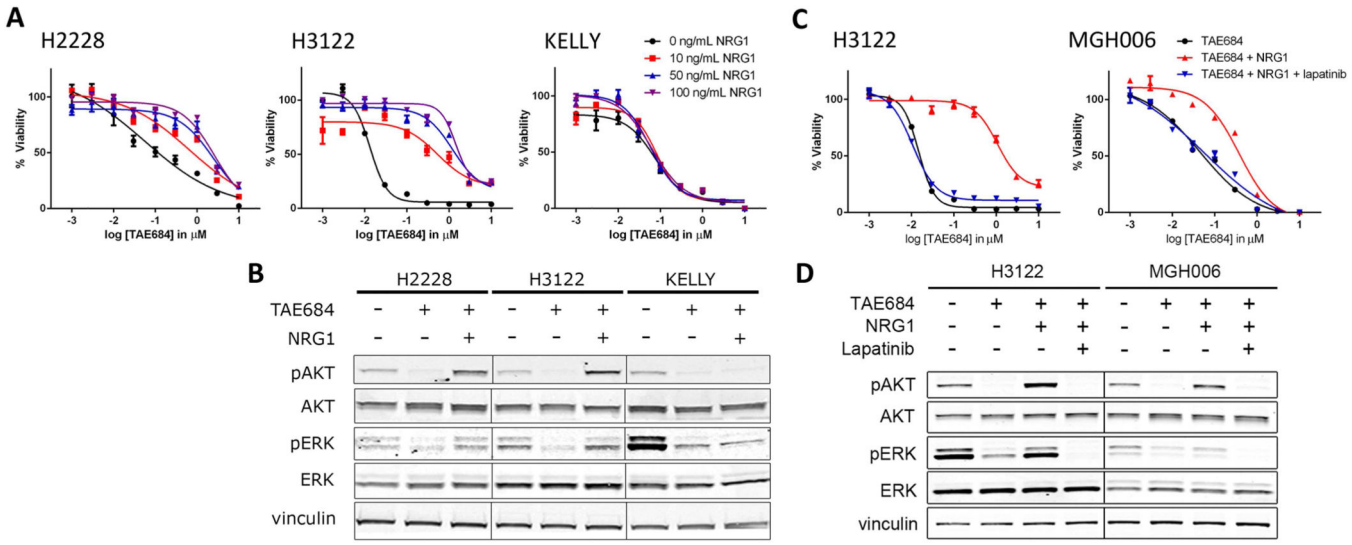

Figure 5.

Neuregulin-1 (NRG1) drives resistance to ALK inhibition in ALK-dependent NSCLC cell lines but not in an ALK-dependent neuroblastoma cell line (KELLY). **A.** H2228, H3122, and KELLY cells were exposed to increasing concentrations of NRG1 at the indicated doses of TAE684 for 5 days. Cell viability was determined with Cell Titer-Glo. Mean and standard error of 3 replicates are shown. **B.** H2228, H3122, and KELLY cells were exposed to 200 nM TAE684 in the presence or absence of 50 ng/mL NRG1 for 6 hours. Immunoblotting of cell lysates was performed with the indicated antibodies. **C.** H3122 and MGH006 cells were exposed to 50 ng/mL NRG1 with or without 1 μM lapatinib in varying concentrations of TAE684 for 5 days. Cell viability was determined as in A. Mean and standard error of 3 replicates are shown. **D.** H3122 and MGH006 cells were exposed to combinations of 200 nM TAE684, 50 ng/mL NRG1, and 1 μM lapatinib for 6 hours. Immunoblotting was performed using the indicated antibodies.

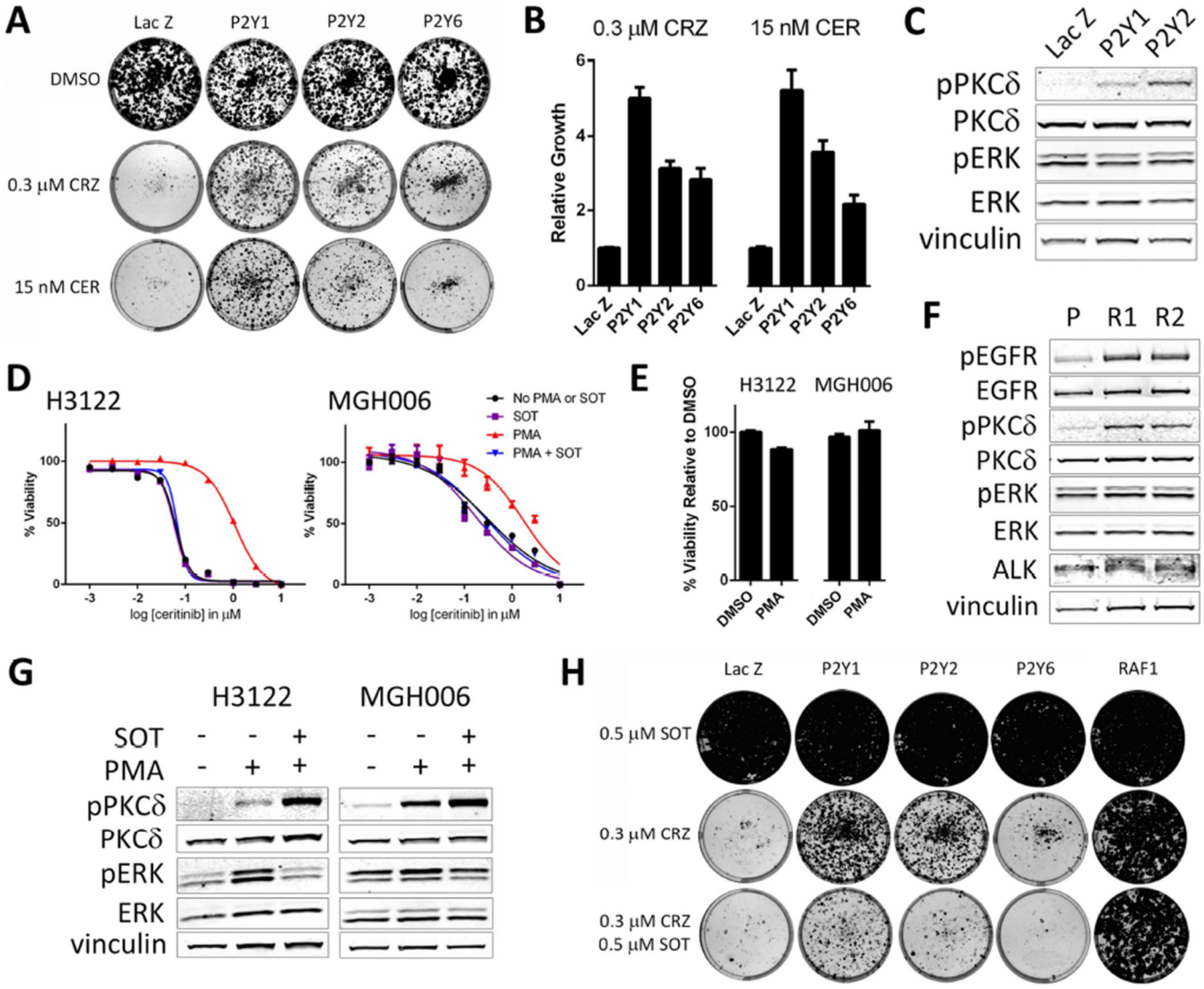

Figure 6.

P2Y receptors drive resistance to ALK Inhibition in H3122 via a PKC-dependent mechanism. **A.** H3122 expressing Lac Z, P2Y1, P2Y2, or P2Y6 were exposed to DMSO for 14 days or 0.3 μM crizotinib (CRZ) or 15 nM ceritinib (CER) for 21 days followed by staining with crystal violet. Media was changed with fresh drug addition every 3 days. **B.** Quantitation of crystal violet uptake by ORF-expressing cells exposed to crizotinib (CRZ) or ceritinib (CER) normalized to Lac Z. Mean and standard error are shown for 6 (CRZ) or 4 (CER) independent experiments of 3 replicates each. **C.** Lysates from H3122 cells overexpressing Lac Z, P2Y1, or P2Y2 were subjected to fractionation and immunoblotting with the indicated antibodies. **D.** H3122 and MGH006 cells were treated with the indicated compounds [1 μM PMA, 0.3 μM sotrastaurin (SOT), or combination] in varying concentrations of ceritinib. Cell viability was determined after 5 days. Mean and standard error of 3 replicates are shown. Results are representative of 4 independent experiments with ceritinib or TAE684. **E.** Cell viability of H3122 and MGH006 treated with 1 μM PMA (normalized to H3122 or MGH006 treated with DMSO as 100%). Mean and standard error

of 3 replicates are shown. The experiment was performed 4 times. **F.** Lysates from parental (P) or ceritinib-resistant (R1, R2) H3122 cells were subjected to fractionation and immunoblotting with the indicated antibodies. **G.** Lysates from H3122 and MGH006 cells treated with 1 μM PMA in the presence or absence of 0.3 μM sotrastaurin (SOT) were fractionated. Immunoblotting was performed with the indicated antibodies. **H.** As in A, except ORF-expressing cells were exposed to the indicated compounds for 20 days. Results are representative of 3 independent experiments. See also Figure S4.

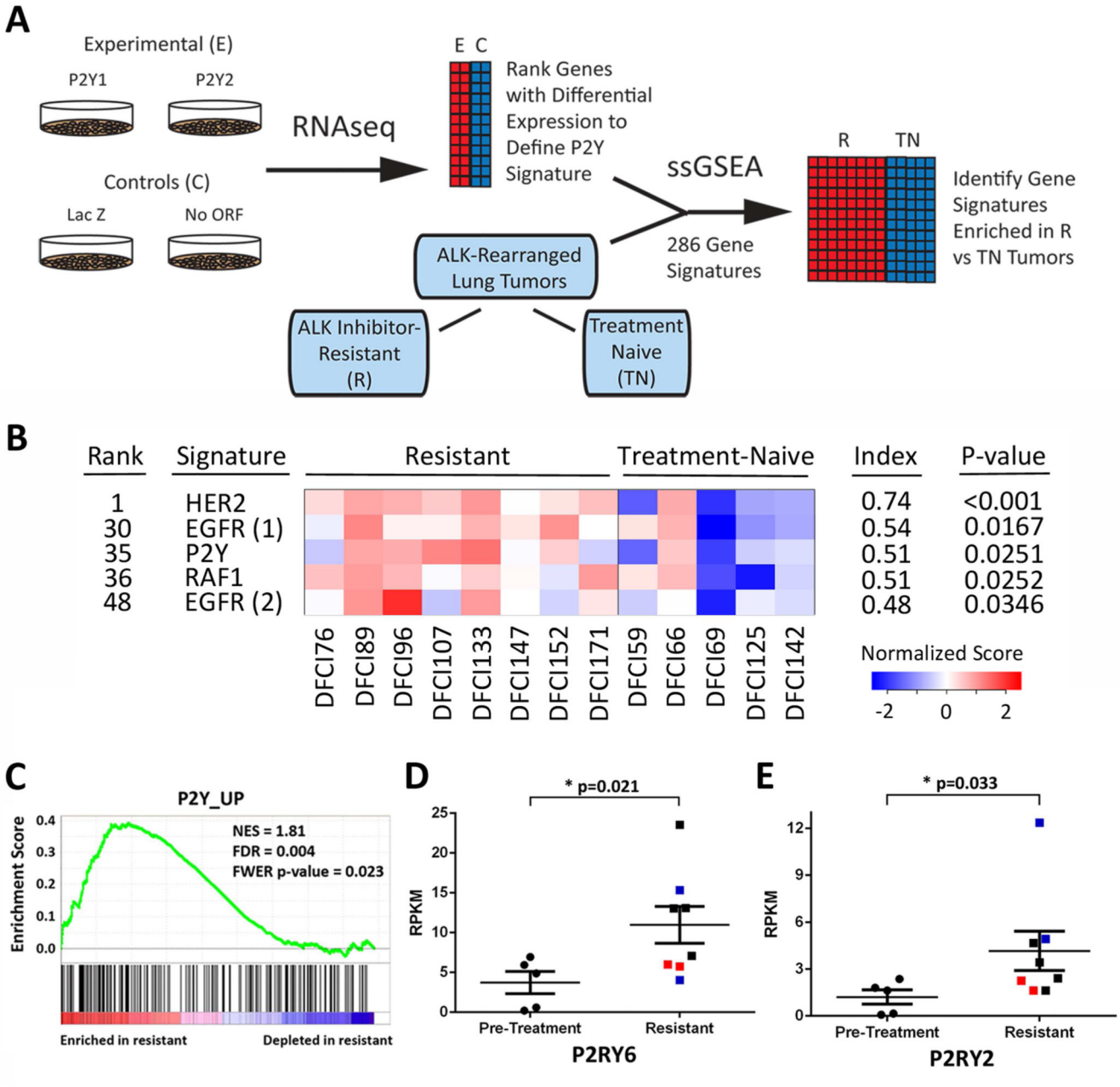

Figure 7.

Enrichment of gene expression signatures in ALK inhibitor-resistant ALK-positive lung tumors compared to treatment-naive ALK-positive lung tumors. **A.** Overview of the experimental approach to generate a P2Y gene signature *in vitro* and to then query this signature (along with 285 additional gene signatures) for enrichment in ALK inhibitor-resistant ALK-rearranged lung tumors compared to treatment-naïve controls. ssGSEA, single-sample gene set enrichment analysis. **B.** Identification of 5 gene signatures enriched in resistant tumors compared to treatment-naïve using ssGSEA. Two independent EGFR signatures were identified; EGFR (1) and EGFR (2) are reported in Creighton et al., 2006 and Gatza et al., 2010, respectively. Index values range from −1 to 1 and refer to correlation

between the indicated gene set and enrichment in resistant compared to treatment-naïve tumors (see Experimental Procedures). Rank positions according to index value for gene signatures (out of 286 total signatures) are indicated. P-values were determined using a permutation test with 1000 permutations of the indicated profile (see Experimental Procedures). **C.** Gene set enrichment analysis reveals that 76 of the top 200 genes up-regulated in the P2Y gene signature (P2Y_UP) are also up-regulated in ALK inhibitor-resistant tumors compared to treatment-naive tumors. NES, normalized enrichment score; FDR, false discovery rate; FWER p-value, family-wise error rate p-value. **D.** Expression of *P2RY6* from RNA-seq of treatment-naive (”pre-treatment”) and ALK inhibitor-resistant (”resistant”) tumors. Expression is indicated in ‘reads per kilobase per million reads’ (RPKM). Mean and standard error are shown. ALK inhibitor-resistant tumors obtained from the same patient are indicated in red or blue. P-value determined by one-tailed Mann-Whitney nonparametric test. **E.** As in D, except for *P2RY2*. See also Figure S5 and Tables S1–S4.

Table 1

Clinical Characteristics of Patient-Derived Tumors

Sample	Age	Gender	Biopsy Site	Status	Response	PFS (Months)	ALK Mutation
DFCI76	63	F	Lymph Node	R	PR	2.8	Yes (L1152R)
DFCI89 *	46	M	Lung Core	R	PR	14	No
DFCI96 *	46	M	Pleural Fluid	R	PR	14	No
DFCI107 **	41	F	Liver Metastasis	R	PR	6.4	No
DFCI133 **	41	F	Liver Metastasis	R (ceritinib)	SD	7.4	No
DFCI147	61	M	Lung Core	R	PR	9.8	No
DFCI152	67	F	Lung Core	R	PR	33.5	No
DFCI171	58	M	Pleural Fluid	R	PR	3.4	No
DFCI59	40	M	Lymph Node	TN	N/A	N/A	No
DFCI66	63	F	Lymph Node	TN	N/A	N/A	No
DFCI69	46	F	Lymph Node	TN	N/A	N/A	No
DFCI125	58	M	Pleural Fluid	TN	N/A	N/A	No
DFCI142	47	M	Pleural Fluid	TN	N/A	N/A	No

Tumor samples derived from the same patient are indicated with * or **.

R = resistant to crizotinib. DFCI133 was obtained after development of resistance first to crizotinib followed by ceritinib. TN = treatment-naïve.
PR, SD = partial response, stable disease (respectively) by RECIST criteria.
PFS = progression-free survival

Tumors harboring secondary ALK mutations known to be associated with crizotinib resistance are indicated under “ALK Mutation”.